

Thermal dependence of photo-induced effects in spin-coated As₂₀Ge_{12.5}S_{67.5} thin films

Stanislav Slang¹, Karel Palka^{1,2*}, Miroslav Vlcek¹

¹Center of Materials and Nanotechnologies, Faculty of Chemical Technology, University of Pardubice, Pardubice 532 10, Czech Republic

²Department of General and Inorganic Chemistry, Faculty of Chemical Technology, University of Pardubice, Pardubice 532 10, Czech Republic

* karel.palka@upce.cz

Abstract

Chalcogenide glass thin films of ternary As₂₀Ge_{12.5}S_{67.5} composition were prepared in specular quality using spin-coating technique from n-butylamine based glass solution. The content of organic residuals was notably reduced by post-deposition thermal treatment. The annealing process induced significant structural changes resulting in thin films with the structure close to the source bulk glass. The thickness of deposited thin films was decreasing with increasing annealing temperature. Contrary, the refractive index, optical bandgap, roughness and chemical stability were increasing. The experimental data also proved that deposited thin films were photo-sensitive as opto-physical properties and chemical resistance were changed after UV light exposure. The exposed thin films annealed below 90°C were etched slower than unexposed ones (negative etching) and the thin films annealed above 90°C were etched faster (positive etching).

Introduction

Chalcogenide glasses (ChGs) are promising optical materials due to their unique properties such as wide IR transmission window or high values of refractive index [1-7]. Metastability of the glass structure often results in photo-sensitivity of ChG (in dependence on the composition, form and history of the sample) [1-4], which can lead to selective etching of exposed and unexposed areas in suitable etching solutions [8-11].

ChG are frequently used in a form of a thin film. ChG thin films are usually deposited by physical vapor deposition techniques such as vacuum thermal evaporation, laser ablation or sputtering [1-7]. Alternatively, the solution based deposition techniques which exploit the solubility of ChG in volatile organic amines are also gaining attention [10-16]. On laboratory level scale the spin-coating technique is commonly used but other related techniques (e.g. spiral bar coating, electrospray) have been proven suitable as well [17]. The solution based deposition techniques are simple and cheap due to the lack of need for high vacuum equipment (contrary to the physical vapor deposition methods). Their major disadvantage is the content of organic residuals in the thin films which can be significantly reduced by proper post-deposition thermal treatment [11-15].

ChG thin films are often photo-sensitive, but the origin of their sensitivity is dependent on the used deposition technique [1, 5, 6, 7, 11]. Photo-induced changes of thin films deposited from ChG solutions usually significantly differ from those of thin films prepared by vacuum thermal evaporation as was demonstrated in [10]. The photo-sensitivity of ChG thin films deposited from amine based solutions is mainly connected with the presence of organic ChG salts (organic amine molecules ionically bonded to the ChG nano-clusters [11-13]) formed during the glass dissolution process. The ChG salts are also present in deposited thin film matrix and they can be gradually decomposed with increasing annealing temperature [10-16]. Hence the photo-sensitivity of the thin films prepared by solution based deposition techniques is also affected by post-deposition annealing [10, 11].

In presented work, we report on the thermal dependence of photo-induced effects in spin-coated As₂₀Ge_{12.5}S_{67.5} thin films induced by UV light exposure. The glass composition was

chosen as combination of previously thoroughly studied $As_{40}S_{60}$ and $Ge_{25}S_{75}$ glass compositions [10, 11, 14]. Photo- and thermo-induced changes of optical properties, surface roughness, chemical resistance, elemental composition and thin film structure were studied in this work and the issue of Ge-containing spin-coated ChG thin films is discussed.

Experimental

The source bulk $As_{20}Ge_{12.5}S_{67.5}$ chalcogenide glass was synthesized using standard melt-quenching method. Pure 5N elements were loaded in appropriate amounts into quartz ampule and sealed under vacuum ($\sim 10^{-3}$ Pa). The glass synthesis was carried out in rocking tube furnace for 72 hours with peak temperature $950^{\circ}C$. Subsequently, the quartz ampule with melted glass was quenched in a cold water.

Bulk glass was powdered in agate bowl and dissolved in n-butylamine (BA) solvent with concentration of 0.075 g of glass powder per 1 ml of BA resulting in clear solution without any precipitate or turbidity. Glass solution was pipetted onto rotating soda-lime glass substrates and spin-coated (Best Tools SC110) at 2000 rpm in Ar inert atmosphere for 120 s. Deposited thin films were immediately stabilized by annealing at $60^{\circ}C$ for 20 min on a hot plate (Conbrio, Czech Republic) to remove excess BA solvent. Stabilized samples are hereinafter referred as as-prepared thin films. Thin films were stored in dark dry environment at laboratory temperature.

As-prepared thin films were annealed at 75, 90, 105, 120, 135, 150, 165 and $180^{\circ}C$ for 60 min on the hot plate inside argon-filled annealing chamber. The as-prepared and annealed thin film samples were exposed to the UV lamp (365 nm main peak, $137 \text{ mW}\cdot\text{cm}^{-2}$) for 60 min inside argon-filled exposure chamber.

Transmission spectra of studied thin films were measured using UV-VIS-NIR optical spectrometer (Shimadzu UV3600) in spectral region 190-2000 nm. Surface roughness of spin-coated samples was determined according to the ISO 4287/1 norm using atomic force microscope (Solver NEXT, NT-MDT, Russia) equipped with NSG10 (NT-MDT, Russia) measuring tips. The spectra and AFM measurements were always performed on three samples with the same treatment.

The compositions of the as-prepared, annealed and exposed thin films were analyzed by energy dispersion x-ray microanalysis method using scanning electron microscope (LYRA 3, Tescan, Czech Republic) equipped with EDS analyzer Aztec X-Max 20 (Oxford Instruments) at acceleration voltage 5 kV.

Chemical stability of thin film samples was studied using wet-etching technique. Spin-coated thin films were etched in 1 vol.% BA solution in aprotic solvent (N,N-dimethylformamide) at $25^{\circ}C$ and etching kinetics were determined by procedure presented in [18].

Structure of source bulk glass and studied thin films was determined by FT-IR spectrometer IFS55 with Raman module FRA106 (Bruker) using Nd:YAG excitation laser (1064 nm). The Raman spectra were recorded with laser beam intensity of 150 mW (2 cm^{-1} resolution, 200 scans) and normalized by intensity of the most intense band in the spectrum.

Results and discussion

Transmission spectra of studied $As_{20}Ge_{12.5}S_{67.5}$ thin films were evaluated by the procedure described in [10] based on the thin film transmission spectrum model published by Swanepoel in [19] and refractive index parametrization model published by Wemple & DiDomenico [20]. The quality of fit was determined as residual sum of squares (RSS) between fitted and experimental spectrum. The RSS of fitted data didn't exceed the value of 0.06 (within fitted transparent region ~ 1200 nm). The typical fitted spectrum of as-prepared and annealed thin

film together with Tauc's plot are presented in Figure 1. Provided data of optical parameters and thickness represent the average values of three measurements and the error bars stand for the standard deviation of calculated values.

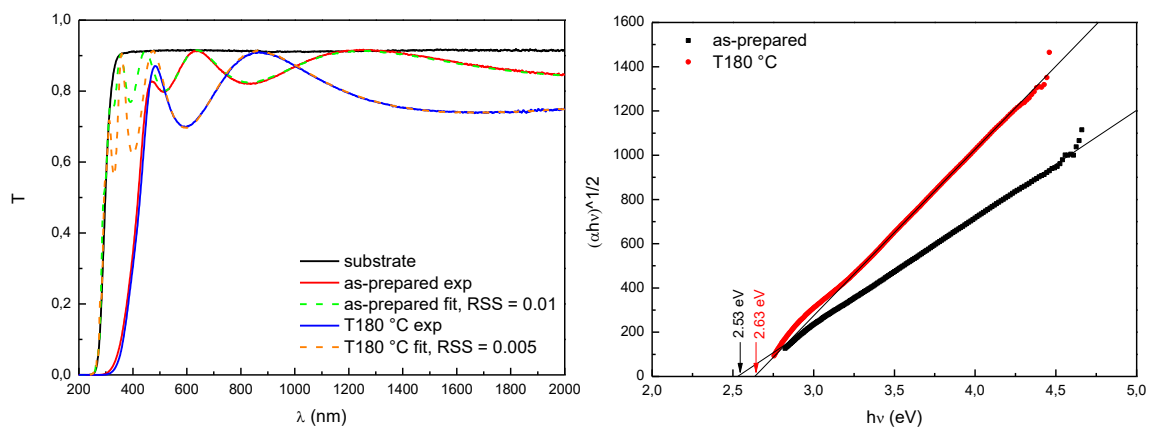


Fig. 1. The measured and fitted transmission spectra (left) and Tauc's plots (right) of as-prepared and annealed spin-coated $As_{20}Ge_{12.5}S_{67.5}$ thin films (exp – experimental data, fit – fitted data, RSS – residual sum of squares in fitted transparent region).

The thickness of the as-prepared thin films was ~ 340 nm. Annealing process of the as-prepared thin films induced significant thickness decrease (Figure 2). The thickness of thin film annealed at $180^{\circ}C$ was about ~ 200 nm which corresponds to 59% of the original films thickness.

Observed phenomenon can be explained by presence of solvent residuals in the matrix of as-prepared thin films [10-16]. BA solvent residuals are present either as chemically bonded or free encapsulated molecules [11, 15]. With increasing annealing temperature, the free BA molecules are released and solvent-containing micellar-like glass nanoclusters in form of alkyl ammonium arsenic sulfide (AAAS) and alkyl ammonium germanium sulfide (AAGS) salts start to decompose [11, 15]. This process is usually accompanied by structural polymerization and films densification which result in observed thickness decrease. The data proved that UV exposure of the thin films has no significant influence on films thickness.

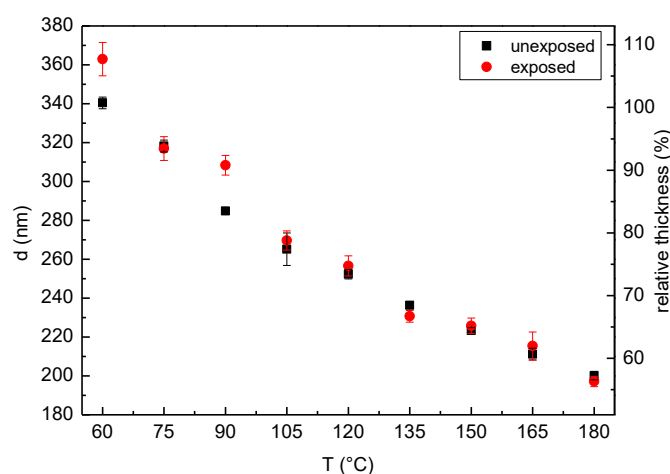


Fig. 2 Thermal dependence of the $As_{20}Ge_{12.5}S_{67.5}$ spin-coated thin films thickness.

The surface roughness of both unexposed and exposed thin films was studied using AFM in semicontact mode. Obtained scans were evaluated according to the ISO 4287/1 norm

providing the root mean square (RMS) values of the surface roughness. The values of surface roughness of thermally stabilized thin films are increasing with increasing annealing temperature (Figure 3). It has been proved that Ge-Sb-S thin films are nano-porous with cavities closed on the film surface [14]. Based on data provided in [14] we can assume that similar cavities are also present in Ge-containing $As_{20}Ge_{12.5}S_{67.5}$ spin-coated thin films and together with significant thermo-induced thickness decrease contributing to the observed increase in surface roughness. Thin films annealed at temperatures $\leq 120^{\circ}C$ exhibit low surface roughness ≤ 1 nm with no significant difference between unexposed and exposed thin films. Contrary, the thin films annealed at temperatures higher than $120^{\circ}C$ have significantly higher surface roughness with their values up to ~ 7 nm. The UV light exposure of thin films annealed at temperatures higher than $120^{\circ}C$ resulted in decrease of their surface roughness. The structural features on AFM scans of unexposed and exposed thin films annealed at $180^{\circ}C$ given in Figure 4 verify observed phenomena. The surface of exposed thin film is significantly smoother with lower content of surface “blisters”. Although we cannot yet sufficiently explain observed exposure induced roughness decrease, the effect of exposure is eminent.

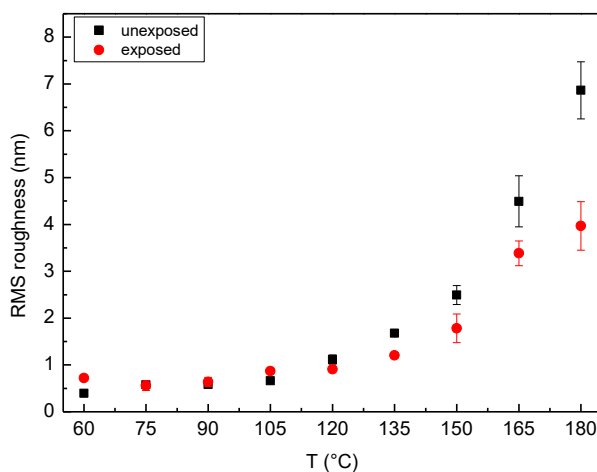


Fig. 3 The dependence of surface roughness on annealing temperature of $As_{20}Ge_{12.5}S_{67.5}$ spin-coated thin films.

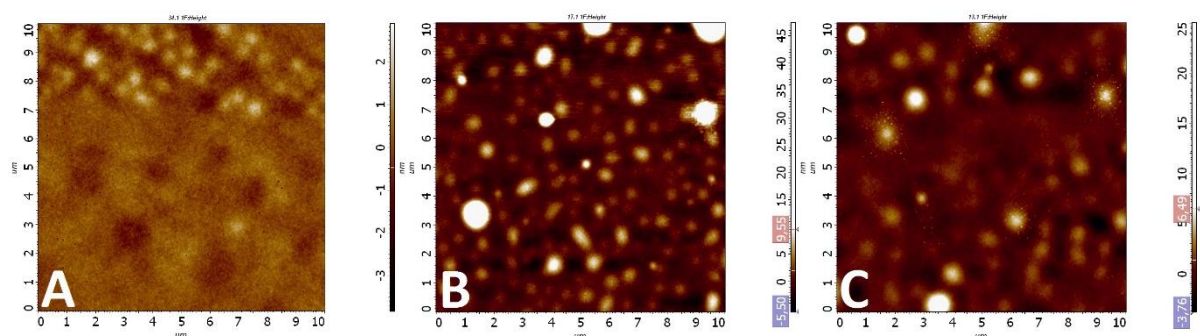


Fig. 4 AFM scans of as-prepared thin film (A) together with unexposed (B) and exposed (C) thin films annealed at $180^{\circ}C$ of $As_{20}Ge_{12.5}S_{67.5}$ composition.

Glass densification and structural changes induced by increasing temperature during thermal stabilization resulted in homogeneous increase in refractive index (Figure 5). The refractive index n_{1550} ($\lambda = 1550$ nm) of as-prepared spin-coated $As_{20}Ge_{12.5}S_{67.5}$ thin films is 1.83 which is higher than refractive index as-prepared spin-coated Ge-S thin film [15] but lower than refractive index of as-prepared spin-coated As-S thin film [11, 21]. The UV light exposure of as-prepared and annealed thin films always induced refractive index decrease but

the effect of irradiation is decreasing with increasing annealing temperature. The refractive index decrease is more eminent on thin film samples annealed below 105°C. At this temperature, the AAAS salts are almost completely decomposed [11-13] and AAGS salts are just starting to decompose [15].

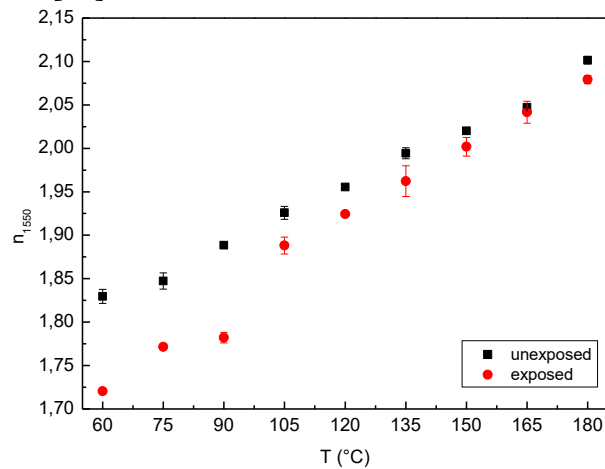


Fig. 5 The dependence of refractive index n_{1550} ($\lambda = 1550$ nm) on the annealing temperature of $As_{20}Ge_{12.5}S_{67.5}$ spin-coated thin films.

The optical bandgap values were calculated using Tauc's model for amorphous semiconductors [22] from measured transmission spectra. The optical bandgap of studied samples is monotonously increasing with increasing annealing temperature up to at 120°C (Figure 6). No further significant change of E_g^{opt} can be observed on thin film samples annealed at higher temperatures. The UV light exposure induced decrease of the optical bandgap (photo-darkening). No significant photo-induced changes of optical bandgap were reported on spin-coated As-S thin films [11] which indicates that the content of Ge-S structural units increases the photo-sensitivity of deposited glass material.

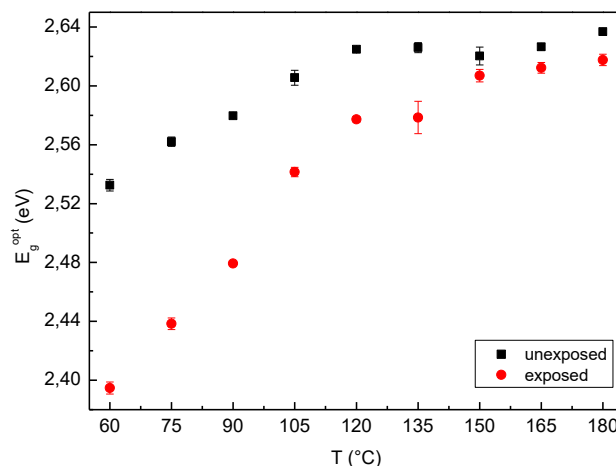


Fig. 6 The dependence of the optical bandgap (E_g^{opt}) on annealing temperature of $As_{20}Ge_{12.5}S_{67.5}$ spin-coated thin films.

Chemical resistance of unexposed and exposed $As_{20}Ge_{12.5}S_{67.5}$ thin films was studied by their etching in 1% vol. BA solution in an aprotic solvent – N,N-dimethylformamide (Figure 7 – left). The etching rates of unexposed thin films are decreasing with increasing annealing temperature which indicates increase in chemical stability, especially for samples annealed above 105°C. The structure of annealed thin film is more polymerized as AAAS salts are mostly decomposed at this temperature and thin film structure is more densified [11]. Higher

annealing temperatures did not cause any significant decrease of the etching rates. The UV exposure of thin films annealed at 60°C (as-prepared) and 75°C resulted in decrease of the etching rates, i.e. exposed samples were dissolved slower than unexposed ones (negative etching). Contrary, thin films annealed at temperatures above 75°C showed positive etching – exposed samples were dissolved faster than unexposed ones. Temperature dependence of the etching selectivity (ratio of the etching rate of exposed and unexposed thin film) is given in Fig. 7 (right). Maximum etching selectivity was observed on the samples annealed at 135°C.

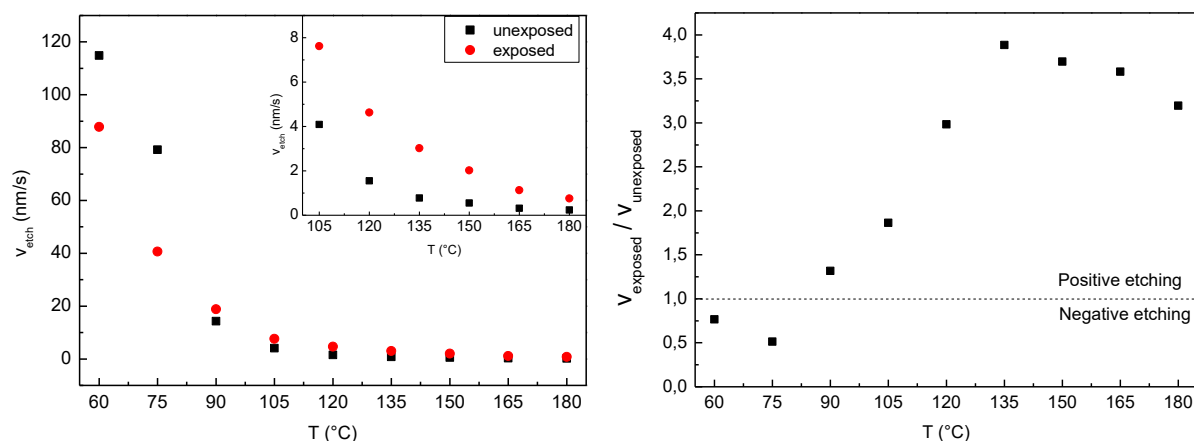


Fig. 7 The etching rates (left) of unexposed and exposed $As_{20}Ge_{12.5}S_{67.5}$ spin-coated thin films and their etching selectivity (right).

The structure of source bulk glass and thin film samples was studied by Raman spectroscopy (Figure 8). The main structural units of source ternary $As_{20}Ge_{12.5}S_{67.5}$ bulk glass are $AsS_{3/2}$ trigonal pyramidal units with main band at 344 cm^{-1} [23-25] and $GeS_{4/2}$ corner-shared tetrahedral units with band at 340 cm^{-1} [26-28] sharing almost the same position and thus they both are contributing to high intensity of the main Raman band. The shoulder at 367 cm^{-1} can be attributed to the symmetric vibrations of $AsS_{3/2}$ trigonal pyramidal units [29]. The presence of broad low-intensive shoulder at 430 cm^{-1} confirms that the structure of source bulk glass also comprises $GeS_{4/2}$ edge-shared tetrahedral pyramidal units [27, 28]. Due to the over-stoichiometry of sulfur the bands at 475 and 495 cm^{-1} can be found in measured Raman spectrum. They can be attributed to vibrations of S_8 rings (475 cm^{-1}) [24, 30, 31] and S-S chains (495 cm^{-1}) [24, 31].

The structure of as-prepared spin-coated $As_{20}Ge_{12.5}S_{67.5}$ thin film is very different from the source bulk glass (Figure 8, compare curves 1 and 10). The main structural units are also $AsS_{3/2}$ trigonal pyramidal units and $GeS_{4/2}$ corner-shared tetrahedral units, but the $GeS_{4/2}$ band is much sharper suggesting lower level of their structural polymerization. Similar shape of sharp $GeS_{4/2}$ band was already observed in the Raman spectrum of as-prepared spin-coated $Ge_{25}S_{75}$ thin film [15]. The sharp bands at 151 , 218 and 475 cm^{-1} can be attributed to the vibrations of S_8 rings indicating their higher concentration in comparison with the source bulk glass. The Raman band of arsenic rich realgar-like As_4S_4 cages vibration at 369 cm^{-1} also appears in measured spectrum [10, 25, 32]. As it was mentioned earlier, the dissolution of chalcogenide glasses in aliphatic amines results in formation of ionic organic-chalcogenide compounds. The bands at $2800 - 3000\text{ cm}^{-1}$ prove that the deposited thin films contain residual BA molecules [11, 33]. Three additional wide bands at 191 , 415 and 455 cm^{-1} can be identified in measured Raman spectrum of as-prepared sample and they can be assigned to vibrations of AAAS (415 cm^{-1}) [11, 33] and AAGS (191 and 455 cm^{-1}) [15] salt residuals.

The annealing process induces structural changes (Figure 8 – left) in two separated thermal regions given by the decomposition temperatures of As- and Ge-based salts. The structural

polymerization of As-based structural units is induced by annealing at lower temperatures and at 105°C it is practically completed [11]. The intensities of AAAS salt band at 415 cm⁻¹ and BA molecules band at 2800 – 3000 cm⁻¹ are reduced with increasing annealing temperature. The bands of As₄S₄ structural units (369 cm⁻¹) and S₈ rings (151, 218 and 475 cm⁻¹) are also decreasing with increasing annealing temperature. The wide band of AsS_{3/2} trigonal pyramidal units vibration at 344 cm⁻¹ is proportionally increasing. It is in a good agreement with observed structural polymerization of As-S spin-coated thin films [10-13]. Annealing above 120°C induces structural polymerization of Ge-based structural units [15] with observed decomposition of AAGS salts (bands 191 and 455 cm⁻¹ disappearing) and gradual releasing of additional BA molecules. It should be also noted that annealing at elevated temperatures was done in one temperature step so the decomposition of AAAS and AAGS salts occurred simultaneously and probably both As and Ge structural units were subsequently bonded together. The structure of thin film annealed at 165°C is very similar to the structure of source bulk glass, but the fluorescence band starts to interfere with Raman spectrum. In case of sample annealed at 180°C the fluorescence significantly exceeds films Raman signal and thus make the spectrum difficult to evaluate.

The Raman spectra proved that UV exposure has significant influence on the structure of as-prepared spin-coated As₂₀Ge_{12.5}S_{67.5} thin film (Figure 8 – right), but the nature of these structural changes differs from that observed on As-S thin films [11]. The UV exposure of as-prepared As₃₀S₇₀ thin film induces structural polymerization comparable with structural changes induced by annealing. In case of as-prepared As₂₀Ge_{12.5}S_{67.5} thin film structural changes are more complicated as As- and Ge-based structural units react slightly differently to UV light exposure. The AAAS (415 cm⁻¹) and AAGS (191 and 455 cm⁻¹) salts are both decomposed and portion of residual BA molecules is released (reduced intensity 2800 – 3000 cm⁻¹). The S dangling bonds which originated from thermal decomposition of ChG salts reacts with arsenic rich As₄S₄ structural units (369 cm⁻¹) resulting in disappearance of their bands from measured spectrum and formation of AsS_{3/2} trigonal pyramidal units [10-13]. Moreover, some portion of S atoms is probably released during the salt decomposition and start to form S₈ rings (151, 218 and 475 cm⁻¹) which was also observed on Ge-Sb-S spin-coated thin films [14] and results suggest that this phenomenon is probably connected with AAGS salt residuals. Thus, the structure of exposed as-prepared sample becomes more polymerized which explains its observed higher chemical stability. With increasing annealing temperature of unexposed thin film, the content of organic residuals is gradually decreasing, the structure of thin film is more compact and polymerized which result in observed decreasing of exposure induced structural changes. But similarly to As-S spin-coated thin films, the UV exposure of As-Ge-S spin-coated thin films probably induces formation of structural defects which increase the intensity of luminescence background and subsequently decrease films chemical stability [10, 11].

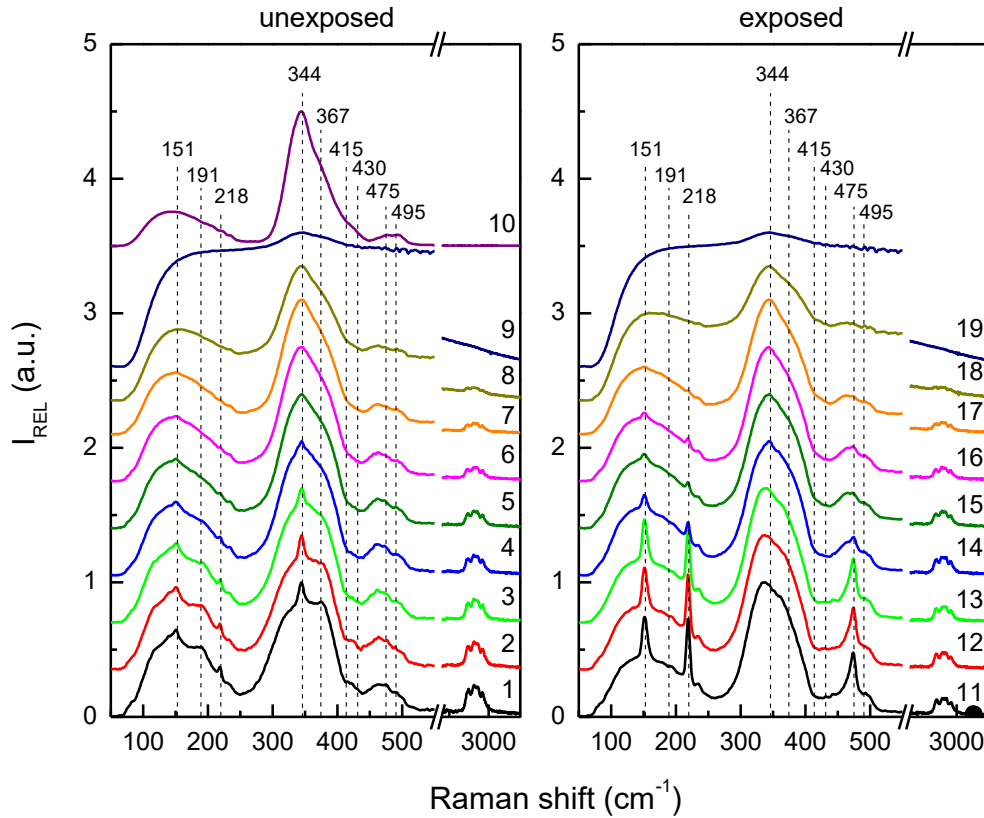


Fig. 8 The Raman spectra of $As_{20}Ge_{12.5}S_{67.5}$ bulk glass and spin-coated thin film samples. 1 – as-prepared thin film, 2 – annealed at $75^{\circ}C$, 3 – annealed at $90^{\circ}C$, 4 – annealed at $105^{\circ}C$, 5 – annealed at $120^{\circ}C$, 6 – annealed at $135^{\circ}C$, 7 – annealed at $150^{\circ}C$, 8 – annealed at $165^{\circ}C$, 9 – annealed at $180^{\circ}C$, 10 – source bulk glass, 11 – exposed as-prepared thin film, 12 – annealed at $75^{\circ}C$ exposed, 13 – annealed at $90^{\circ}C$ exposed, 14 – annealed at $105^{\circ}C$ exposed, 15 – annealed at $120^{\circ}C$ exposed, 16 – annealed at $135^{\circ}C$ exposed, 17 – annealed at $150^{\circ}C$ exposed, 18 – annealed at $165^{\circ}C$ exposed, 19 – annealed at $180^{\circ}C$ exposed.

The effect of annealing and light irradiation on the thin films composition was investigated using elemental analysis by EDS. The results confirm that the As-Ge-S content of deposited thin films is not significantly changing during annealing (Figure 9). The composition of thin film annealed at $180^{\circ}C$ is $As_{20}Ge_{12}S_{68}$ which is in a good agreement with planned $As_{20}Ge_{12.5}S_{67.5}$ composition. The UV exposure also slightly affects the As-Ge-S content as the as-prepared thin film and thin films annealed up to $150^{\circ}C$ exhibit minor S depletion (~ 1.5 at.%). Similar phenomenon was reported on $Ge_{23}Sb_7S_{70}$ spin-coated samples [14] and together with the irradiation induced formation of S_8 rings proves that this effect is common for different Ge containing spin-coated ChG thin films.

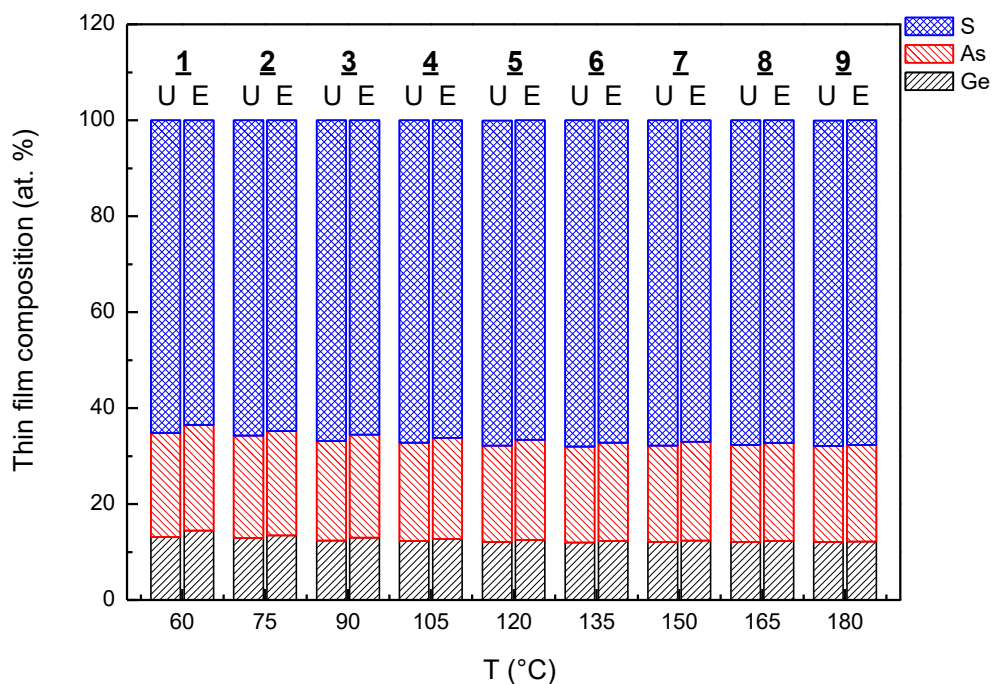


Fig. 9 The As-Ge-S content of unexposed (U) and exposed (E) spin-coated thin films. 1 – as-prepared thin film, 2 – annealed at 75°C, 3 – annealed at 90°C, 4 – annealed at 105°C, 5 – annealed at 120°C, 6 – annealed at 135°C, 7 – annealed at 150°C, 8 – annealed at 165°C, 9 – annealed at 180°C.

The content of organic residuals in the thin films was also studied by EDS. The organic molecules content was investigated using the concentration of nitrogen atoms. The BA molecule contains one nitrogen atom and no other source of nitrogen in the studied thin films can be expected. Thus, the nitrogen atomic content should be equivalent to the content of organic residual molecules bonded inside the glass matrix. The nitrogen content in unexposed and exposed samples is given relative to the content of arsenic (Figure 10). The obtained data proved decreasing content of organic residuals in thin film matrix with increasing annealing temperature, especially after annealing above 105°C when the start of AAGS salts decomposition is expected. The UV exposure has also distinctive influence on the organic residuals content. The thin film samples annealed below 135°C exhibit significant loss of nitrogen-containing molecules supporting the proposed mechanism of irradiation induced salt decomposition. With increasing annealing temperature, the glass matrix is more polymerized and more compact, thus no irradiation induced nitrogen decrease is observed on samples annealed above 135°C.

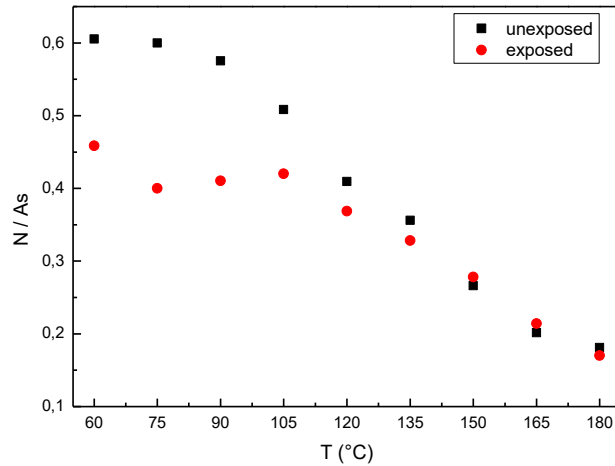


Fig. 10. Dependence of N:As atomic ratio on annealing temperature measured by EDS technique.

The presented data of optical parameters, structural analysis and elemental composition show that UV exposure of spin-coated $\text{As}_{20}\text{Ge}_{12.5}\text{S}_{67.5}$ thin films induced changes of thin film parameters unlike the ones, which are usually observed on thin films deposited using physical vapor deposition methods (e.g. vacuum thermal evaporation, laser ablation etc.) [1-4]. Especially, the refractive index is usually decreasing as optical bandgap is increasing (or vice versa) after exposure of photo-sensitive chalcogenide thin films being exposed to the appropriate light source. In our case, both the refractive index and optical bandgap are decreasing after UV light exposure. This phenomenon is more eminent on the samples annealed below 120°C . This anomalous behavior can be explained by completely different photo-induced structural changes of studied spin-coated thin films. Photo-sensitive thin films prepared by physical vapor deposition techniques are usually changing only the bond rearrangement within the material upon the illumination [1-4]. Contrary, the spin-coated thin films are losing the material of organic residuals (Figure 10) besides the significant structural changes (Figure 8) during UV light exposure – thus the change in spin-coated thin films is not only structural but compositional as well. As the temperature of annealing is increasing, the content of organic residuals is decreasing and subsequently the effect of UV illumination is decreased.

Conclusion

The experimental data proved that ternary $\text{As}_{20}\text{Ge}_{12.5}\text{S}_{67.5}$ thin films can be deposited by spin-coating technique in specular optical quality. Similarly to the other spin-coated chalcogenide glass thin films, their physical and chemical properties are significantly changing with increasing of annealing temperature. Observed thermo-induced thickness decrease is accompanied by increase in films refractive index, optical bandgap and surface roughness. These changes are connected to observed structural polymerization of thin film glass matrix and releasing of organic residuals resulting in increase of their chemical stability.

Deposited $\text{As}_{20}\text{Ge}_{12.5}\text{S}_{67.5}$ thin films are also photo-sensitive. UV-light exposure induced structural changes connected with decrease of their refractive index and optical bandgap. The etching kinetics proved that the etching selectivity is changing with the increase of annealing temperature. The exposed thin films annealed below 90°C are etched slower than unexposed ones (negative etching) and contrary the thin films annealed above 90°C have inversed selectivity (positive etching). The Raman spectroscopy and EDS elemental analysis confirmed

that UV exposure induces decomposition of alkyl ammonium arsenic sulfide and alkyl ammonium germanium sulfide salts and releasing of n-butylamine molecules.

Acknowledgments

Authors appreciate financial support from project No. 16-13876S financed by the Grant Agency of the Czech Republic (GA CR) as well as support from the grants LM2015082 and CZ.1.05/4.1.00/11.0251 from the Ministry of Education, Youth and Sports of the Czech Republic.

References

- [1] K. Tanaka, K. Shimakawa, *Amorphous Chalcogenide Semiconductors and Related Materials*, Springer (2011) New York.
- [2] Z. Borisova, *Glassy Semiconductors*, Plenum Press (1981) New York.
- [3] K. Tanaka, M. Mikami, *Phys. Status Solidi C* 8 (2011) 2756–2760.
- [4] L. Tichy, H. Ticha, P. Nagels, R. Callaerts, *Mater. Lett.* 36 (1998) 294–298.
- [5] R. M. Almeida, L. F. Santos, A. Simens, A. Ganjoo, H. Jain, *J. Non-Cryst. Solids* 18–21 (2007) 2066–2068.
- [6] P. Knotek, J. Navesnik, T. Cernohorsky, M. Kincl, L. Tichy, *Mater. Res. Bull.* 64 (2015) 42–50.
- [7] E. Baudet, C. Cardinaud, A. Girard, E. Rinnert, V. Nazabal, *J. Non-Cryst. Solids* 444 (2016) 64–72.
- [8] A. Stronski, M. Vlcek, A. Sklenar, *Quant. Electron. Optoelectron.* 3 (2000) 394–399.
- [9] J. Orava, T. Wagner, M. Krbal, T. Kohoutek, M. Frumar, *J. Non-Cryst. Solids* 13–15 (2007) 1441–1445.
- [10] K. Palka, S. Slang, J. Buzek, M. Vlcek, *J. Non-Cryst. Solids* 447 (2016) 104–109.
- [11] S. Slang, K. Palka, H. Jain, M. Vlcek, *J. Non-Cryst. Solids* 457 (2017) 135–140.
- [12] G. Chern, I. Lauks, *J. Appl. Phys.* 53 (1982) 6979–6982.
- [13] G. Chern, I. Lauks, A.R. McGhie, *J. Appl. Phys.* 54 (1983) 4596–4601.
- [14] M. Waldmann, J. D. Musgraves, K. Richardson, C.B. Arnold, *J. Mater. Chem.* 22 (2012) 17848–17852.
- [15] S. Slang, P. Janicek, K. Palka, M. Vlcek, *Opt. Mater. Express* 6(6) (2016) 1973–1985.
- [16] S. Song, N. Carlie, J. Boundies, L. Petit, K. Richardson, C. B. Arnold, *J. Non-Cryst. Solids* 355 (2009) 2272–2278.
- [17] K. Palka, T. Syrový, S. Schröter, S. Brückner, M. Rothardt, M. Vlcek, *Opt. Mater. Express* 4 (2014) 384–395.
- [18] L. Loghina, K. Palka, J. Buzek, S. Slang, M. Vlcek, *J. Non-Cryst. Solids* 430 (2015) 21–24.
- [19] R. Swanepoel, *J. Phys. E: Sci. Instrum.* 16 (1983) 1214–1222.
- [20] S. H. Wemple, M. DiDomenico, *Physical Review B* 3 (1971) 1338–1351.
- [21] E. Hajto, P. J. S. Ewen, R. Belford, J. Hajto, A. E. Owen, *J. Non-Cryst. Solids* 97&98 (1987) 1191–1194.
- [22] J. Tauc, *Mater. Res. Bull.* 3 (1968) 37–46.
- [23] R. Ston, Mir. Vlcek, H. Jain, *J. Non-Cryst. Solids* 236 (2003) 220–225.
- [24] M. Pisarcik, L. Koudelka, *Mater. Chem.* 7 (1982) 499–507.
- [25] R. Holomb, V. Mitsa, O. Petrachenkov, M. Veres, A. Stronski, M. Vlcek, *Phys. Status Solidi* 8 (2011) 2705–2708.
- [26] K. Tanaka, M. Yamaguchi, *J. Non-Cryst. Solids* 227–230 (1998) 757–760.
- [27] T. Haizheng, Z. Xiujiang, J. Chengbin, *J. Mol. Struct.* 697(1–3) (2004) 23–27.
- [28] H. Guo, H. Tao, Y. Zhai, S. Mao, X. Zhao, *Spectrochim. Acta A Mol. Biomol. Spectrosc.* 67(5) (2007) 1351–1356.

- [29] J. D. Musgraves, P. Wachtel, B. Gleason, K. Richardson, *J. Non-Cryst. Solids* 386 (2014) 61–66.
- [30] T. Cardinal, K. A. Richardson, *J. Non-Cryst. Solids* 256&257 (1999) 353–360.
- [31] Z. Cernosek, J. Holubova, E. Cernoskova, A. Ruzicka, *J. Non-oxide Glas.* 1 (2009) 38–42.
- [32] J. Tasseva, R. Todorov, Tz. Babeva, K. Petkov, *J. Opt.* 12 (2010) 065601 (9pp).
- [33] S. Slang, K. Palka, L. Loghina, A. Kovalskiy, H. Jain, M. Vlcek, *J. Non-Cryst. Solids* 426 (2015) 125–131.